ISSN 1063-7761, Journal of Experimental and Theoretical Physics, 2007, Vol. 105, No. 3, pp. 479–485. © Pleiades Publishing, Inc., 2007.
Original Russian Text © V.I. Balykin, V.G. Minogin, 2007, published in Zhurnal Éksperimental'noĭ i Teoreticheskoĭ Fiziki, 2007, Vol. 132, No. 3, pp. 543–550.

ATOMS, MOLECULES, OPTICS

Focusing of an Atomic Beam by a Fresnel Atom Microlens

V. I. Balykin and V. G. Minogin*

Institute of Spectroscopy, Russian Academy of Sciences, Troitsk, Moscow oblast, 142190 Russia
**e-mail: minogin@isan.troitsk.ru*

Received February 6, 2007

Abstract—Focusing of an atomic beam by a Fresnel atom microlens formed by an optical field diffracted by an aperture whose size is comparable to or greater than the radiation wavelength is considered. It is shown that the dipole gradient force enables one to focus the atomic beam to a spot of about 10 nm in diameter. The focusing properties of a Fresnel atom microlens are analyzed within a model describing the dipole interaction of rubidium atoms with monochromatic radiation near the *D*-line.

PACS numbers: 32.80.Pj, 42.50.Vk

DOI: 10.1134/S1063776107090026

1. INTRODUCTION

In recent years, considerable attention has been given to the development of methods for focusing atomic beams by spatially inhomogeneous laser fields. These methods are based on the use of dipole gradient forces that pull atoms into regions of maximum field intensity when the field frequency is red-detuned with respect to the atomic transition frequency. The development of these methods made it possible to focus atomic beams by a Gaussian laser beam [1, 2], hollow laser beams [3–8], standing waves of laser radiation [9–17], as well as by specially formed rather complex axially symmetric fields [18, 19]. The approaches developed have already been employed not only in atom optics but also in micro- and nanofabrication of materials, as well as in atomic lithography with nanometer resolution [20–22].

Another, as yet poorly studied, approach to the focusing of atomic beams is the application of atom microlenses formed by the optical field diffracted by small apertures in metallic screens [23–25]. A unique feature of this approach is the possibility of creating, on the basis of a single screen, a large number of atom microlenses and, hence, the possibility of forming a large number of atomic microbeams from a single beam. The characteristic feature of this approach is the use of a gradient force in a spatial domain of size comparable to or less than the size of the microaperture, rather than in the focusing region of a laser beam or in a region with a size of about the radiation wavelength. Accordingly, atom microlenses may produce atomic microbeams of very small diameter, and a set of atom microlenses can be used for fabricating microstructures on a substrate.

We can point out two basic types of atom microlenses, which are based on the diffraction of light by small apertures in screens. One of these types relates to the case, considered by Bethe, when the size of the aperture in the screen is less than the radiation wavelength. The second case is similar to the Fresnel diffraction, when the size of the aperture is comparable to or greater than the light wavelength. Until now, the scheme of atomic focusing has been considered only in the case of Bethe diffraction [23–25]. The analysis carried out has shown that efficient focusing can be achieved for a relatively slow atomic beam. For large velocities of atoms, the focusing capability of the laser near-field zone is restricted due to the small interaction time between atoms and the laser field.

In the present paper, we carry out a quantitative analysis of the focusing properties of a Fresnel atom microlens. The analysis of the properties of a Fresnel atom microlens is based on the application of the Rayleigh–Sommerfeld diffraction integral to the case of diffraction of electromagnetic fields by a circular aperture. We investigate the distribution of laser radiation in the near-field diffraction zone, obtain an analytic representation for the field near the optical axis, and calculate the gradient force near the aperture in the screen when the size of the aperture is comparable to or greater than the radiation wavelength. We use an estimate of the gradient force for the numerical analysis of the trajectories of atoms in the near-field Fresnel zone of an atom microlens and for finding analytic estimates for the parameters of the microlens.

2. ELECTROMAGNETIC FIELD

In the scheme of a Fresnel atom microlens shown in Fig. 1, a laser field illuminates a screen with a microaperture whose radius a is comparable to or greater than the light wavelength. An atomic beam is incident upon

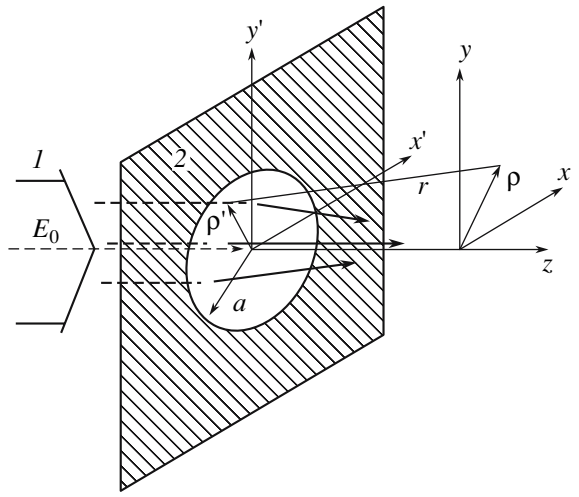

Fig. 1. Fresnel atom microlens based on a diffracted optical field: (*1*) laser radiation incident upon the screen with an aperture, and (*2*) a focused atomic beam.

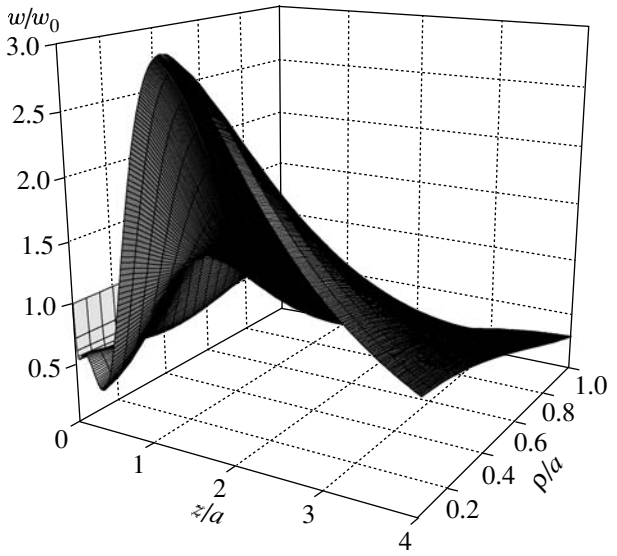

Fig. 2. Electric energy density w of diffracted optical radiation as a function of coordinates z and ρ for an aperture radius of $a = 1.3\lambda$. The energy density w is normalized by the density of the energy of incident radiation $w_0 = E_0^2/16\pi$.

the screen with aperture; this beam is focused by the gradient force due to the inhomogeneous transverse distribution of the diffracted electromagnetic field.

We will assume that the screen with the aperture is illuminated by a plane traveling light wave

$$\mathbf{E}_1 = \mathbf{e}E_0\cos(kz - \omega t), \tag{1}$$

where $\mathbf{e}$ is the unit polarization vector, E_0 is the amplitude, and $k = \omega/c$ is the wave vector of radiation. The intensity of the incident wave (1) is $I = cE_0^2/8\pi$. The electric field of the diffracted wave can be expressed as

$$\mathbf{E}_2 = \mathbf{e}E = \mathbf{e}\mathrm{Re}(\mathscr{E}e^{-i\omega t}), \tag{2}$$

where $\mathscr{E} = \mathscr{E}(\mathbf{r})$ is the complex amplitude of the field. To determine the diffracted electromagnetic field, we apply the Rayleigh–Sommerfeld diffraction formula, which takes account of the boundary conditions in the Kirchhoff approximation. According to this formula, the complex electric vector of the diffracted field is given by

$$\mathscr{E}(x, y, z) = \frac{1}{2\pi}\iint\mathscr{E}(x', y', 0)\frac{\exp(ikr)}{r} \times\frac{z}{r}\left(\frac{1}{r} - ik\right)dx'dy', \tag{3}$$

where

$$r = [z^2 + (x - x')^2 + (y - y')^2]^{1/2} \tag{4}$$

is the distance between a point $(x', y', 0)$ in the plane of the aperture and the observation point (x, y, z); the field amplitude in the plane of the aperture is $\mathscr{E}(x', y', 0) = E_0$, and that outside the aperture is $\mathscr{E}(x', y', 0) = 0$.

The distribution of the field diffracted by a circular aperture is axially symmetric. Using convenient cylindrical coordinates ρ', ϕ' and ρ, ϕ, we can rewrite the original formula for the electric field as

$$\mathscr{E}(\rho, z) = \frac{E_0}{2\pi}\int_0^a\int_0^{2\pi}\frac{\exp(ikr)}{r}\frac{z}{r}\left(\frac{1}{r} - ik\right)d\varphi\rho'd\rho', \tag{5}$$

where now

$$r = [z^2 + \rho^2 + \rho'^2 - 2\rho\rho'\cos\varphi]^{1/2}, \tag{6}$$

$\varphi = \phi' - \phi$ is the relative angular coordinate of two points, and a is the aperture radius.

The time-average energy density of the diffracted electric field is given by

$$w = \frac{1}{8\pi}\langle E^2\rangle_t = \frac{1}{16\pi}|\mathscr{E}|^2. \tag{7}$$

A typical three-dimensional profile of the energy density of the diffracted electric field is shown in Fig. 2. Note that, when the aperture size is slightly greater than the radiation wavelength, as in Fig. 2, the distribution of the electric energy density has a pronounced transverse profile with a maximum on the optical axis. This fact shows that the optical field can play the role of an atom lens if the frequency of the field is detuned below the atomic transition frequency; i.e., for negative detuning, the gradient force is directed to the optical axis of the field. Note also that, according to the Kirchhoff approx-

imation, the density w of the electric energy of the diffracted field inside the aperture coincides with the density of electric energy of the incident radiation, $w_0 = E_0^2/16\pi$.

Along with the integral representation (5), one can also obtain an analytic representation for the electric field, which is valid for small deviations ρ from the optical axis. To determine the latter deviation, we expand the integrand in Eq. (5) in a series in powers of a small displacement $\rho \ll a$. To take into account, in addition to the focusing effect of the atom lens, the aberrations of the lens, we perform the expansion up to fourth-order terms in ρ. In this approximation, we obtain the following expression for the distance between the point of radiation and the point of observation of the field:

$$r = R - \frac{\rho'\cos\varphi}{R}\rho + \frac{1}{2R}\left(1 - \frac{\rho'^2\cos^2\varphi}{R^2}\right)\rho^2 + \frac{\rho'\cos\varphi}{2R^3}\left(1 - \frac{\rho'^2\cos^2\varphi}{R^2}\right)\rho^3 - \frac{1}{8R^3}\left(1 - \frac{6\rho'^2\cos^2\varphi}{R^2} + \frac{5\rho'^4\cos^4\varphi}{R^4}\right)\rho^4, \quad (8)$$

where $R = (z^2 + \rho'^2)^{1/2}$. Then, expanding the integrand in formula (5) up to fourth-order terms in ρ, we can integrate with respect to the angular coordinate φ. After that, we can pass from integration with respect to the coordinate ρ' to integration with respect to the coordinate R, and thus reduce the double integral in (5) to a single integral:

$$\mathcal{E}(\rho, z) = -E_0\int_z^{R_a} dR e^{ikR}\left(\frac{ikz}{R}A - \frac{z}{R^2}B + \frac{9ikz\rho^2}{4R^3}C - \frac{9z\rho^2}{4R^4}D - \frac{15ikz^3\rho^2}{4R^5}E + \frac{15z^3\rho^2}{4R^6}F - \frac{525ikz^3\rho^4}{32R^7}G + \frac{525z^3\rho^4}{32R^8}H + \frac{945ikz^5\rho^4}{64R^9} - \frac{945z^5\rho^4}{64R^{10}}\right). \quad (9)$$

Here, $R_a = (z^2 + a^2)^{1/2}$, and the following functions of the coordinates of the observation point are introduced:

$$A = 1 - \frac{1}{4}k^2\rho^2 + \frac{1}{64}k^4\rho^4,$$

$$B = 1 - k^2\rho^2 + \frac{7}{64}k^4\rho^4,$$

$$C = 1 + \frac{1}{9}k^2z^2 - \frac{11}{48}k^2\rho^2 - \frac{1}{72}k^4z^2\rho^2,$$

$$D = 1 + \frac{2}{3}k^2z^2 - \frac{3}{4}k^2\rho^2 - \frac{11}{72}k^4z^2\rho^2,$$

$$E = 1 - \frac{15}{16}\frac{\rho^2}{z^2} - \frac{13}{24}k^2\rho^2 - \frac{1}{240}k^4z^2\rho^2,$$

$$F = 1 - \frac{15}{16}\frac{\rho^2}{z^2} - 2k^2\rho^2 - \frac{1}{16}k^4z^2\rho^2,$$

$$G = 1 + \frac{1}{10}k^2z^2,$$

$$H = 1 + \frac{2}{5}k^2z^2.$$

Expression (9) can be calculated by integrating by parts. Then, we can obtain the following analytical expression for the complex electric field amplitude:

$$\mathcal{E}(\rho, z) = E_0\mathcal{J}, \quad (10)$$

where the function $\mathcal{J}$ relating the diffracted and incident fields,

$$\mathcal{J} = e^{ikz}\left(1 - \frac{z}{R_a}e^{ik(R_a - z)}\right) + \frac{k^2a^2z\rho^2}{4R_a^3}\left(1 + \frac{3i}{kR_a} - \frac{3}{k^2R_a^2}\right)e^{ikR_a} - \frac{k^4a^4z\rho^4}{64R_a^5}\left[1 + \frac{2i(3 - 2z^2/a^2)}{kR_a} - \frac{3(7 - 8z^2/a^2)}{k^2R_a^2} - \frac{15i(3 - 4z^2/a^2)}{k^3R_a^3} + \frac{15(3 - 4z^2/a^2)}{k^4R_a^4}\right]e^{ikR_a}, \quad (11)$$

is valid up to fourth-order terms in the small coordinate ρ. Note that, in the plane of the aperture, i.e., for $z = 0$, the diffracted field coincides with the incident field, and hence $\mathcal{J} = 1$. When $\rho = 0$, the analytic formula obtained reduces to the formula obtained in the papers [26, 27], where the authors investigated an analytic expression for the electric field on the optical axis of the system, i.e., in the zero order with respect to the transverse coordinate ρ. Note also that, although we used the Kirchhoff–Sommerfeld approximation to estimate the diffracted optical field, which does not reproduce the exact boundary conditions of the diffraction problem, it is well known that the Rayleigh–Sommerfeld formula quite satisfactorily describes all values of the field, including those in the near-field zone [28–30].

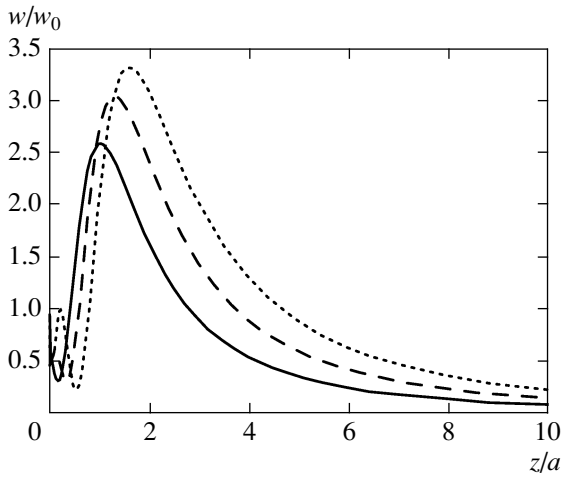

Fig. 3. Electric energy density on the optical axis of a Fresnel microlens for an aperture radius of $a = \lambda$ (solid line), 1.3λ (dashed line), and 1.6λ (dotted line).

Using formula (11), we can also obtain an analytic expression for the electric energy density (7) for small distances from the optical axis,

$$w = w_0 \mathcal{J}, \tag{12}$$

where the function $\mathcal{J}$ is defined up to fourth-order terms in powers of the displacement ρ:

$$\begin{aligned}\mathcal{J} &= 1 + \frac{z^2}{R_a^2} - \frac{2z}{R_a}\cos[k(R_a - z)] \\ &- \frac{k^2 a^2 z \rho^2}{2R_a^3}\left[\left(1 - \frac{3}{k^2 R_a^2}\right)\left(\frac{z}{R_a} - \cos[k(R_a - z)]\right)\right. \\ &\left. + \frac{3}{kR_a}\sin[k(R_a - z)]\right] \\ &+ \frac{k^4 a^4 z \rho^4}{32R_a^5}\left[\left(1 - \frac{3(7 - 8z^2/a^2)}{k^2 R_a^2} + \frac{15(3 - 4z^2/a^2)}{k^4 R_a^4}\right)\right. \\ &\times\left(\frac{z}{R_a} - \cos[k(R_a - z)]\right) + \frac{1}{kR_a} \\ &\left.\times\left(2\left(3 - 2\frac{z^2}{a^2}\right) - \frac{15(3 - 4z^2/a^2)}{k^2 R_a^2}\right)\sin[k(R_a - z)]\right].\end{aligned} \tag{13}$$

Recall that $w_0 = E_0^2/16\pi = I/2c$ is the density of the electric energy of the incident radiation and I is the intensity of the incident radiation.

The distributions of the electric energy density along and across the optical axis, determined by numerically integrating the Rayleigh–Sommerfeld formula, are shown in Figs. 3 and 4. Figure 3 represents the electric energy density of the diffracted field on the optical axis for various values of the aperture radius in the screen. One can see that, when the aperture radius is on the order of the wavelength of laser radiation, the characteristic scale of the focusing region of the Fresnel atom lens amounts to several wavelengths. Figure 4 represents the transverse distribution of the electric energy density for nine different values of the distance from the screen with aperture. One can see that, at small distances from the screen with aperture, variations of the transverse profile of the field density change the direction of the gradient force. However, starting from the distance $z \approx a$, the transverse profile of the field density has a stable form corresponding to the focusing of atoms for negative frequency detuning.

3. GRADIENT FORCE

The atoms of a microbeam that pass through the aperture in the screen are subject to a dipole force that includes both the dissipative force of light pressure and the gradient force [17, 31]. In the region before the screen, the atoms may be subject to the light pressure force only, which does not play any role in the focusing of the beam. In the region behind the screen, an atomic microbeam can be focused only due to the radial component of the gradient force, which is dominant in the case when the detuning of the frequency of the field with respect to the atomic transition frequency is large. The light pressure force and the longitudinal component of the gradient force, which exist in the same region and are directed along the axis of the beam, are mainly responsible for a small variation in the longitudinal velocity of atoms and can be neglected in the analysis, because, in the atomic beam, the longitudinal components of velocity are much greater than the transverse components.

The radial component of the gradient force when the red-detuning of the frequency of the field with respect to the quantum transition frequency is much greater than both the homogeneous linewidth and the Doppler frequency shift due to the longitudinal velocity of an atom can be expressed in the approximation of a two-level interaction scheme as [17, 31]

$$F_\rho = \frac{\hbar\gamma^2}{2|\delta|}\frac{\partial G}{\partial \rho}. \tag{14}$$

Here, $\delta = \omega - \omega_0$ is the detuning of the frequency of the field with respect to the quantum transition frequency,

$$2\gamma = \frac{4}{3}\frac{d^2\omega^3}{\hbar c^3} \tag{15}$$

is the rate of spontaneous decay of the upper state to the lower ground state,

$$G = \frac{1}{2}\left(\frac{dE}{\hbar\gamma}\right)^2 \tag{16}$$

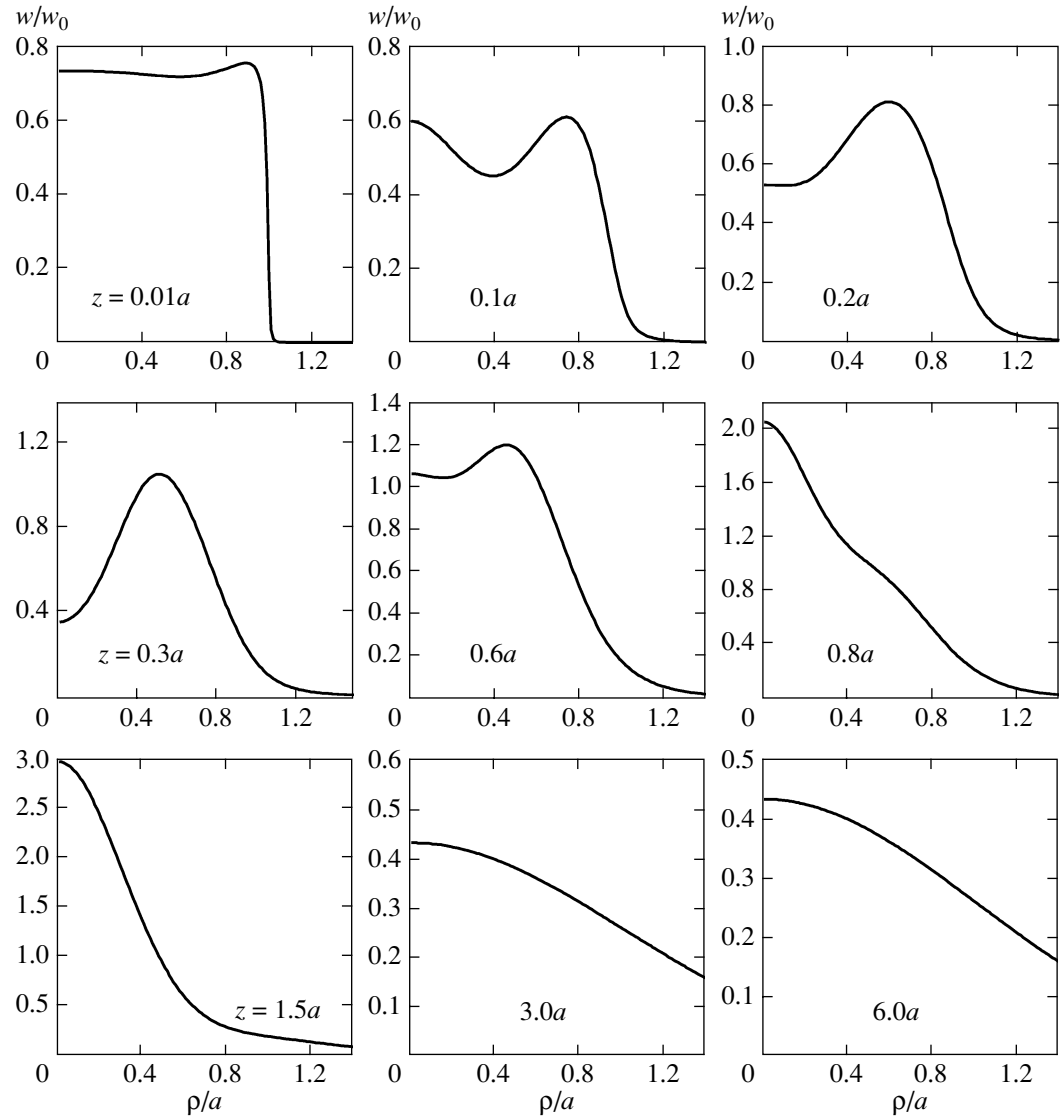

Fig. 4. Electric energy density of a Fresnel microlens as a function of the radial coordinate ρ for an aperture radius of $a = 1.3\lambda$ and for the longitudinal coordinate z as shown in the figures.

is a dimensionless saturation parameter, d is the matrix element of the dipole moment of an atom, and E is the amplitude of the electric field at the location of the atom.

In our paper, it is convenient to express the saturation parameter in terms of the electric energy density,

$$G = \frac{8\pi d^2 w}{\hbar^2 \gamma^2}. \tag{17}$$

Then, the radial component of the gradient force, which we refer to for short as the gradient force, takes the following obvious form:

$$F_\rho = 6\pi \frac{\gamma}{|\delta|} \frac{1}{k^3} \frac{\partial w}{\partial \rho}. \tag{18}$$

For small deviations from the optical axis, we can obtain an analytic estimate for the gradient force (18); this estimate follows from the analytic expression (12) for the density of electric energy near the optical axis. For negative detuning, the gradient force has the form

$$F_\rho = -\kappa(z)\rho + \mu(z)\rho^3, \tag{19}$$

where the elasticity constant κ and the anharmonicity constant μ are functions of the coordinate z,

$$\kappa(z) = \frac{3\pi I}{\omega_0} \frac{\gamma}{|\delta|} \frac{a^2 z}{R_a^3} \left[\left(1 - \frac{3}{k^2 R_a^2}\right) \times \left(\frac{z}{R_a} - \cos[k(R_a - z)]\right) + \frac{3}{kR_a} \sin[k(R_a - z)] \right], \tag{20}$$

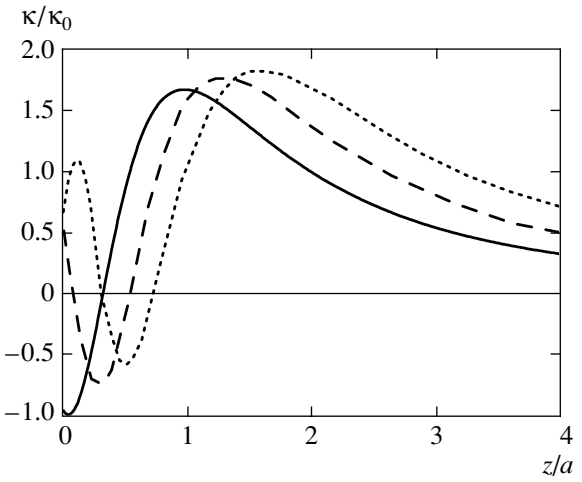

Fig. 5. Normalized elasticity constant κ/κ_0, where $\kappa_0 = (I/3\pi\omega_0)(\gamma/|\delta|)$, as a function of the longitudinal coordinate for an aperture radius of $a = \lambda$ (solid line), 1.3λ (dashed line), and 1.6λ (dotted line).

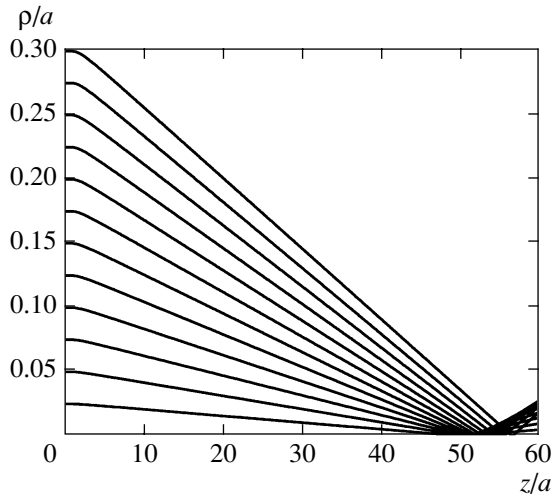

Fig. 6. Trajectories of atoms in the atomic beam focused by a Fresnel atom microlens. A screen with an aperture of radius $a = 1.3\lambda = 1$ μm is irradiated by optical radiation for a mismatch of $\delta = -10^3\gamma$ and intensity $I = 10$ W/cm^2. The longitudinal velocities of atoms in the beam are $V = 10$ m/s.

$$\mu(z) = \frac{3\pi k I}{8c}\frac{\gamma}{|\delta|}\frac{a^4 z}{R_a^5}\left[\left(1 - \frac{3(7 - 8z^2/a^2)}{k^2 R_a^2}\right.\right.$$

$$\left. + \frac{15(3 - 4z^2/a^2)}{k^2 R_a^2}\right)\left(\frac{z}{R_a} - \cos[k(R_a - z)]\right) \qquad (21)$$

$$\left. + \frac{1}{kR_a}\left(2\left(3 - \frac{2z^2}{a^2}\right) - \frac{15(3 - 4z^2/a^2)}{k^2 R_a^2}\right)\sin[k(R_a - z)]\right],$$

$I = (c/8\pi)E_0^2$ is the intensity of the incident radiation, and ω_0 is the frequency of atomic transition.

Formulas (19)–(21), as well as Figs. 2 and 4, show that, immediately behind the screen with aperture, the gradient force may lead to a weak defocusing of the central part of the atomic beam; however, farther from the screen, the gradient force focuses the beam within a much longer part of the trajectory. We can evaluate that, for an aperture size of about the wavelength of radiation, the focusing region is about an order of magnitude greater than the defocusing region. This behavior of the gradient force is illustrated in Fig. 5, which represents the dependence of the elasticity constant as a function of the longitudinal coordinate. When the elasticity constant is negative, the gradient force defocuses the atomic beam, whereas, when this constant is positive, the gradient force focuses the beam.

4. BEAM FOCUSING

Consider, for definiteness, the focusing of a beam of ^{85}Rb atoms interacting with the laser radiation on the strong dipole transition $5^2S_{1/2}(F = 3)$–$5^2P_{3/2}(F = 4)$ with the wavelength $\lambda = 780$ nm. The natural linewidth for this transition is $2\gamma = 2\pi \cdot 5.98$ MHz.

To avoid the possible influence of the edge of the metallic microaperture on the dynamics of atoms with induced dipole moments, we will assume that the external part of the atomic beam is separated by an additional dielectric diaphragm. To illustrate this approach, we show in Fig. 6 the trajectories of ^{85}Rb atoms in a microbeam whose initial radius is restricted by a diaphragm at a value of $0.3a$.

Here, we present analytic estimates, assuming that the size of the aperture in the metallic screen amounts to several wavelengths of laser radiation. According to (20), the value of the focusing gradient force in its active region $z > a$ is equal to

$$F_\rho \approx -\kappa_0 \rho, \qquad (22)$$

where the elasticity constant can be evaluated as

$$\kappa_0 \approx \frac{\pi I}{3\omega_0}\frac{\gamma}{|\delta|} \qquad (23)$$

for an average value of the longitudinal coordinate of $z \approx 3a$. Using this value of the radial force near the optical axis, we can estimate the oscillation frequency of an atom when it passes through the optical field:

$$\Omega \approx \sqrt{\frac{\kappa_0}{M}} = \sqrt{\frac{\pi I}{3M\omega_0}\frac{\gamma}{|\delta|}}, \qquad (24)$$

where M is the mass of the atom. This oscillation frequency leads to the focusing of atomic trajectories with the focal length f determined by the longitudinal velocity $V = v_z$ of atoms and the quarter of the oscillation period,

$$f \approx \frac{\pi V}{2\Omega} = \frac{V}{2}\sqrt{\frac{3\pi M\omega_0|\delta|}{I}}\frac{|\delta|}{\gamma}. \quad (25)$$

In the case of ^{85}Rb atoms under consideration, for a laser radiation intensity of $I = 10$ W/cm^2 and detuning of $\delta = -10^3\gamma$, the oscillation frequency is $\Omega \approx 5.6 \times 10^5$ s^{-1}; for example, for the longitudinal velocity of the atomic beam equal to 10 m/s, the focal length is estimated to be $f \approx 30$ μm, which is only two times smaller than the value obtained from the trajectories of motion determined by the numerical solution of the equations of motion (see Fig. 6).

The main factors that restrict the size of the focal spot seem to be the nonmonochromaticity of the atomic beam, aberrations due to the anharmonicity of the gradient force, and the beam spreading due to the velocity diffusion. Since modern methods of velocity monochromatization allow one to obtain atomic beams with monochromaticity of 10^{-3}–10^{-4}, according to estimate (25), the size of the spot due to the nonmonochromaticity of the focused beam may be on the order of 10 nm. The effect of anharmonicity of the gradient force can be estimated by using the numerical values of the trajectories of atoms shown in Fig. 6. These numerical estimates also give a value of the spot size at the focus on the order of 10 nm. Finally, the contribution of the velocity diffusion to the size of the focal spot turns out to be very small, on the order of fractions of a nanometer, due to the small flight time of atoms through the optical field region.

5. CONCLUSIONS

The analysis carried out has shown that a Fresnel atom microlens can efficiently focus an atomic beam. The focal length of a Fresnel atom microlens is largely determined by the longitudinal velocity of the atomic beam, the intensity of laser radiation, and the detuning of the radiation frequency with respect to the atomic transition frequency. The size of the spot at the focus is mainly determined by the nonmonochromaticity of the atomic beam and by small anharmonicity of the radial component of the gradient force. For realistic parameters of the dipole interaction between atoms and laser radiation, we have found that the focal length of a Fresnel atom microlens may be on the order of 100 μm, while the size of the focal spot of the focused beam may be on the order of 10 nm.

ACKNOWLEDGMENTS

This work was supported in part by the Russian Foundation for Basic Research (project no. 05-02-16370-a) and by the US Civil Research and Development Foundation (project no. RU-P1-2572-TR-04).

REFERENCES

1. J. E. Bjorkholm, R. R. Freeman, A. Ashkin, and D. B. Pearson, Phys. Rev. Lett. **41**, 1361 (1978).
2. J. E. Bjorkholm, R. R. Freeman, A. Ashkin, and D. B. Pearson, Opt. Lett. **5**, 111 (1980).
3. V. I. Balykin and V. S. Letokhov, Opt. Commun. **64**, 151 (1987).
4. V. I. Balykin and V. S. Letokhov, Zh. Éksp. Teor. Fiz. **94** (1), 140 (1988) [Sov. Phys. JETP **67**, 78 (1988)].
5. G. M. Gallatin and P. L. Gould, J. Opt. Soc. Am. B **8**, 502 (1991).
6. J. J. McClelland and M. R. Scheinfein, J. Opt. Soc. Am. B **8**, 1974 (1991).
7. M. Prentiss, G. Timp, N. Bigelow, et al., Appl. Phys. Lett. **60**, 1027 (1992).
8. J. L. Cohen, B. Dubetsky, and P. R. Berman, Phys. Rev. A **60**, 4886 (1999).
9. T. Sleator, T. Pfau, V. Balykin, and J. Mlynek, Appl. Phys. B **54**, 375 (1992).
10. G. Timp, R. E. Behringer, D. M. Tennant, et al., Phys. Rev. Lett. **69**, 1636 (1992).
11. J. J. McClelland, R. E. Scholten, E. C. Palm, and R. J. Celotta, Science **262**, 877 (1993).
12. R. W. McGowan, D. M. Giltner, and S. A. Lee, Opt. Lett. **20**, 2535 (1995).
13. R. Gupta, J. J. McClelland, P. Marte, and R. J. Celotta, Phys. Rev. Lett. **76**, 4689 (1996).
14. R. J. Celotta, R. Gupta, R. E. Scholten, and J. J. McClelland, J. Appl. Phys. **79**, 6079 (1996).
15. U. Drodofsky, M. Drewsen, T. Pfau, et al., Microelectron. Eng. **30**, 383 (1996).
16. M. Mutzel, D. Haubrich, and D. Meschede, Appl. Phys. B **70**, 689 (2000).
17. V. I. Balykin, V. G. Minogin, and V. S. Letokhov, Phys. Rep. **63**, 1429 (2000).
18. B. Dubetsky and P. R. Berman, Phys. Rev. A **58**, 2413 (1998).
19. W. Williams and M. Saffman, physics/0506022.
20. M. K. Oberthaler and T. Pfau, J. Phys.: Condens. Matter **15**, R233 (2003).
21. D. Meschede and H. Metcalf, J. Phys. D: Appl. Phys. **36**, R17 (2003).
22. J. J. McClelland, S. B. Hill, M. Pichler, and R. J. Cellota, Sci. Technol. Adv. Matter **5**, 575 (2004).
23. V. Balykin, V. Klimov, and V. Letokhov, J. Phys. II **4**, 1981 (1994).
24. V. I. Balykin, V. V. Klimov, and V. S. Letokhov, Pis'ma Zh. Éksp. Teor. Fiz. **59**, 219 (1994) [JETP Lett. **59**, 235 (1994)].
25. V. I. Balykin, V. G. Minogin, and S. N. Rudnev, Zh. Éksp. Teor. Fiz. **130**, 784 (2006) [JETP **103**, 679 (2006)].
26. H. Osterberg and L. W. Smith, J. Opt. Soc. Am. **51**, 1050 (1961).
27. A. S. Marathay and J. F. McCalmont, J. Opt. Soc. Am. A **21**, 510 (2004).
28. C. L. Andrews, J. Appl. Phys. **21**, 761 (1950).
29. S. Silver, J. Opt. Soc. Am. **52**, 131 (1962).
30. M. Totzeck, J. Opt. Soc. Am. A **8**, 27 (1991).
31. S. Chang and V. Minogin, Phys. Rep. **365/2**, 65 (2002).

Translated by I. Nikitin